Rectification effects of Nafion-backed micropore-voltammograms by difference in migrational modes

Electrochimica Acta 358 (2020) 136839

Contents lists available at ScienceDirect

Electrochimica Acta

journal homepage: www.elsevier.com/locate/electacta

Rectification effects of Nafion-backed micropore-voltammograms by difference in migrational modes

Koichi Jeremiah Aoki[a], Ling Liu[b], Frank Marken[c], Jingyuan Chen[b,*]

[a] Electrochemistry Museum, Fukui 910-0804 Japan
[b] Department of Applied Physics, University of Fukui, 3-9-1, Bunkyo, Fukui-shi 910-0017, Japan
[c] Department of Chemistry, University of Bath, Claverton Down, Bath BA2 7AY, UK

ARTICLE INFO

Article history:
Received 17 May 2020
Revised 25 July 2020
Accepted 25 July 2020
Available online 11 August 2020

Keywords:
Rectification
Pore-voltammograms
Electric migration
Cationic exchange membrane
Asymmetric cell geometry

ABSTRACT

Rectified current-voltage curves were observed by micro-hole voltammetry in various concentrations of sodium ion electrolyte for transport through a micro-hole and a cationic exchange membrane (Nafion). Data suggest a linear current-concentration relation, implying electric migration-control. The rectification is observed as difference in current-potential slopes at positive and at negative applied voltages. The voltammograms are analyzed quantitatively in the context of Ohm's law as a function of both the geometry of the micro-hole and of the entire cell. The conductivity in the direction of the ion transport from the micro-hole to Nafion, corresponding to the lower conductance (closed diode), is proportional both to the cross-section area of the micro-hole and to the inverse micro-hole length. This is consistent with control by electro-migration within the micro-hole. In contrast, the conductivity in the opposite cation transport direction (open diode) is almost independent of the micro-hole geometry but varies with the length of the glass tube of the cell. The current-potential slope is consistent with the value calculated for the NaCl concentration and the geometry of the measurement cell. Under these conditions, the micro-hole is filled with a high concentration of NaCl as the flux of Na^+ from the Nafion to the hole, and the high concentration causes the migration current larger that the current in the opposite direction. Consequently, the rectification ratio can be enhanced by careful design of both (i) the cell geometry including ion-exchange membranes and (ii) the micro-hole geometry rather than nano-scaled chemistry in holes.

1. Introduction

Voltammetry through a nanopore [1–7], a polymer-brush coated cone-pore [8], and conical nano-pores [9–11] has been shown to result in rectified current-voltage curves, which can be related to models for ion channels in living cell membranes. The rectification effects can be industrially applied to electrochemical sensors [3], for desalination [12–16], and for power generation by salt concentration gradient systems [17]. Some efforts have been made to enhancing the rectification ratio by paying specific attention to an increase in asymmetry in shape and functionalization in pores. These include geometrical asymmetry by patterning of cylindrical capillaries [10,18,19], chemical modification by charging sites [9,11], selection of materials of pores [6,20–22], specific voltage control [23], and modification of materials of ionic polymer films [6,24–26]. Improving the rectification ratio is important for future application of ionic diodes.

The ionic rectification through an asymmetrically ionomer-coated micro-hole has been explained in terms of two phenomena: (a) geometric hindrance of the ion transport through the hole for the closed state of the diode associated with localized electrolyte depletion and (b) the localized accumulation of electrolyte giving a highly concentrated ion transport region close to the ion-exchange membrane for the open state of the diode [21,27,28]. In addition, microscopic explanations have often been proposed in terms of "gates" linked to the potential distribution caused by specifically adsorbed ionic moieties in the double-layer or on pore walls [29–35]. Although the concept of "gates" is readily understood, it cannot be applied easily to experimental results in a quantitative manner. Whichever is the dominant rectification mechanism, an asymmetric feature needs to be installed [7,15,24–26,33–38] in a membrane cell based on pore geometry, heterogeneous distribution of ion-associated moieties on pore walls, and/or asymmetric attachment of a semi-permeable membrane on either side

* Corresponding author.
E-mail address: jchen@u-fukui.ac.jp (J. Chen).

https://doi.org/10.1016/j.electacta.2020.136839
0013-4686/

of a micro-hole. The ionic rectification has also been observed for a device composed of a nanopipette coated with surfactants [36–40], which may be included here in terms of geometric asymmetry within pipettes. The rectification has also been found asymmetric nanopores and nanoslots in the context of hydrodynamics [41]. It has been elucidated to be molecular instability in hydrodynamic vortex [42,43], and hence belongs to a category different from the conventional electrochemical behavior.

Quantitative analysis of experimental voltammograms requires a physical model based on electric migration in the light of designing ionic rectifiers with improved pore and cell geometry. If the experimental current is controlled with electric migration of ions in a straight pipe with the cross section area A and length L, the current for the mono-valent cation caused by the voltage V between the two ends of the pipe is expressed by $I = (F^2D/RT)cVA/L$ [44]. Here D and c are the diffusion coefficient and the concentration of the moving cation, respectively. Since this equation demonstrates the proportionality of I to V, it obviously agrees with the experimental results in each half domain of V ($V > 0$ or $V < 0$). However, it fails to express the following properties:

(i) rectification, i.e., dependence of the conductance, I/V, on signs of V,
(ii) geometrically asymmetric variables, and
(iii) ionically interactive variables, including ionic properties on the pore wall.

Property (i) has been partially solved by introducing the dependence of c on V, e.g. c = [in solution bulk] for $V < 0$ and c = [in a cation-semipermeable membrane] for $V > 0$ [45]. However, strong cation-exchange membranes such as Nafion can retain molar order of magnitude of the concentration in milli-molar salt solution in the bulk. Then, the rectification ratio should be up to approx. 1000 times. Unfortunately, experimental results have demonstrated only typical rectification ratio in the order of 10 times. Although property (ii) has been recognized empirically, it may include some other complicated asymmetric features rather than only the asymmetric hole. Property (iii) may result from chemical intuition rather than from geometric features relevant to the electric migration.

In order to clarify problems (i) and (ii), it is necessary to examine conditions of the electric migration in detail by paying attention to the proportionality of I not only to V but also to A, $1/L$, and c. Unfortunately, the dependence on the geometry has not yet been examined in detail, to our knowledge. We should extend our discussion to location-dependence of V, c, and D, including the asymmetry. This work deals with detailed examination of the electric migration through micro-holes with several diameters and lengths by use of Nafion film as a cation exchange membrane. It is shown that in addition to the micro-hole geometry the cell geometry needs to be considered when optimizing the rectification ratio.

2. Experimental

The construction of the cell is shown in Fig. 1(A). Two glass pipes 11.5 mm in inner diameter with ground glass flanges were faced with each other, sandwiching a Nafion film, a pin-holed polyethylene terephthalate (PET) film, and a thin rubber film with a clamp for a ball joint. The Nafion film 0.18 mm thick was purchased from Sigma-Aldrich and was immersed in concentrations of salt for the voltammetric run for one day before voltammetric use. The PET film was drilled commercially with a laser to 10, 20, 30 and 50 μm in diameter. The rubber film worked as avoiding leak of solution. The Nafion film was pressed on the PET film with a vice.

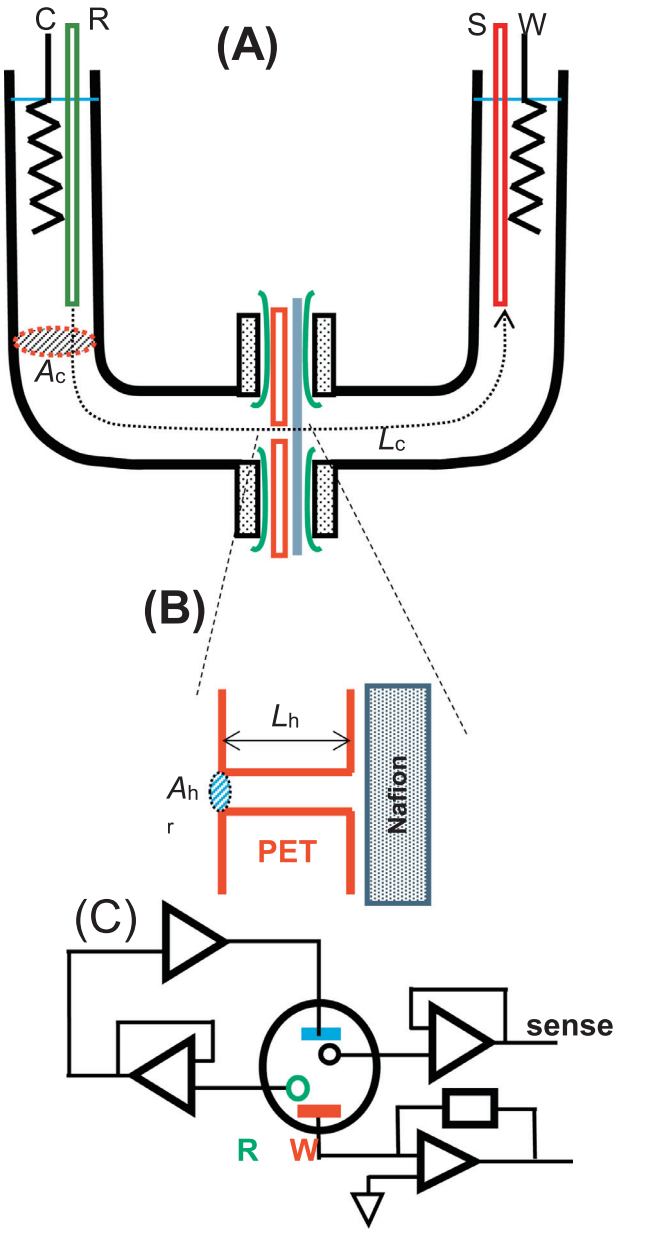

Fig. 1. Illustrations of the structure of the cell (A), the magnified hole (B), and (C) the illustrative circuit of the potentiostat for the sense electrode.

The working electrode and the counter electrode were platinum coils. Potential was detected with a sense electrode and a reference electrode, both of which were silver wires covered with resin except for tips. The tip was coated with AgCl as a local sensor of voltage against the other tip. Taking potential differences avoided fluctuation of compositions of AgCl and concentrations of Cl^-. The current was supplied between the working electrode and the counter electrode, whereas the voltage difference was detected with the sense electrode and the reference electrode by means of the four-electrode system by use of a potentiostat, Compactstat (Ivium, Netherlands).

The resistance of the water-saturated Nafion film was estimated by the ac-impedance technique in the four-electrode system. Two platinum wires were pressed so tightly on the film that the contact did not interfere current supply, whereas two potential sensing AgCl-coated Ag wires were located between the two Pt wires at a given distance.

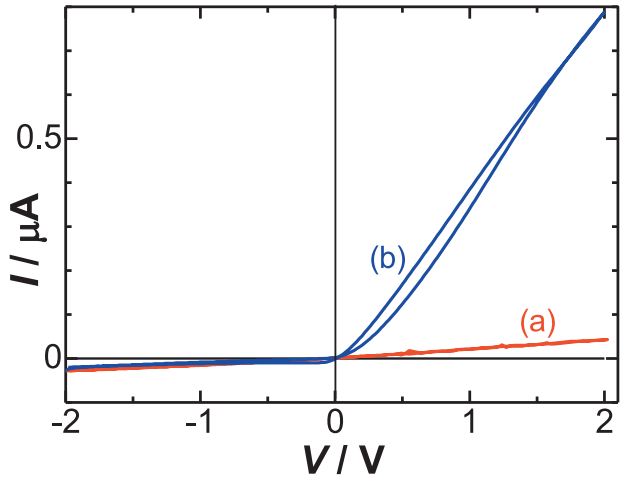

Fig. 2. Typical pore-voltammograms under the 0.1 mM NaCl solution (b) with and (a) without the Nafion film at voltage scan rate 50 mV s^{-1}. The hole geometry was 100 μm long and 20 μm in diameter.

3. Results and discussion

Typical pore-voltammograms with and without Nafion are shown in Fig. 2, from which we can identify some key features:

(i) Voltammograms without Nafion show an ohmic line passing through the origin for all V.
(ii) For data recorded with Nafion for $V > 0$ V and $V < 0$ V each side show a different slope in the current-voltage line.
(iii) The current-voltage slope of the line for $V > 0$ V is larger than that for $V < 0$ V.
(iv) There are only minor scan rate- (v) and potential direction-dependencies in the current-voltage curves for $0.01 < v < 0.15$ V s^{-1}.

These types of observation have been commonly reported also by other researchers for various combinations of ionic exchange membranes, geometric structure of pores, the chemical features of walls of pores, and different kinds of transferring ions. Item (i), i.e. Ohm's law, demonstrates the control of ionically electric migration. Although the linearity of items (ii) and (iii) supports partially the electric migration, it fails to explain significant feature (iii). More explanations are required.

We first examine the voltammograms for $V < 0$. Electric migration occurs not only in the pore but also possibly in the solution bulk, depending on geometry of a passage of transferring ions as well as on the ionic solution composition with low concentration. The resistance of the pore, of the Nafion film, and of the solution can be regarded as a series combination in the geometric structure. Each contribution of the resistance will be examined in turn. Firstly, we tried to estimate the conduction of the Nafion film, and measured voltammograms of the cell separated with and without the Nafion film in 1 M NaCl solution without the PET film. Both the voltammograms observed with/without Nafion film were almost identical with only 2% difference in current, indicating that the Nafion film should have a negligibly small effect on the overall resistivity for pore voltammograms. We evaluated the conductivity of the water-permeated Nafion film by ac-impedance, as described in the experimental section. The Nyquist plots for some separations of the electrodes showed lines, of which intercept to the real part axis provides the resistance. The resistances were proportional to the electrode separation with the coefficient of determination 0.999. The slope provided the resistivity 0.18 Ω m^{-1}, which should be equal to $1/\lambda_{Na}c$ for the molar ionic conductivity of Na^+, λ_{Na}. If λ_{Na} takes the value of aqueous solution, 5.0×10^{-3} S m^2 mol^{-1}, the slope provides $c = 1.1$ M, which makes the resistance of the Nafion film negligibly smaller than the total cell resistance.

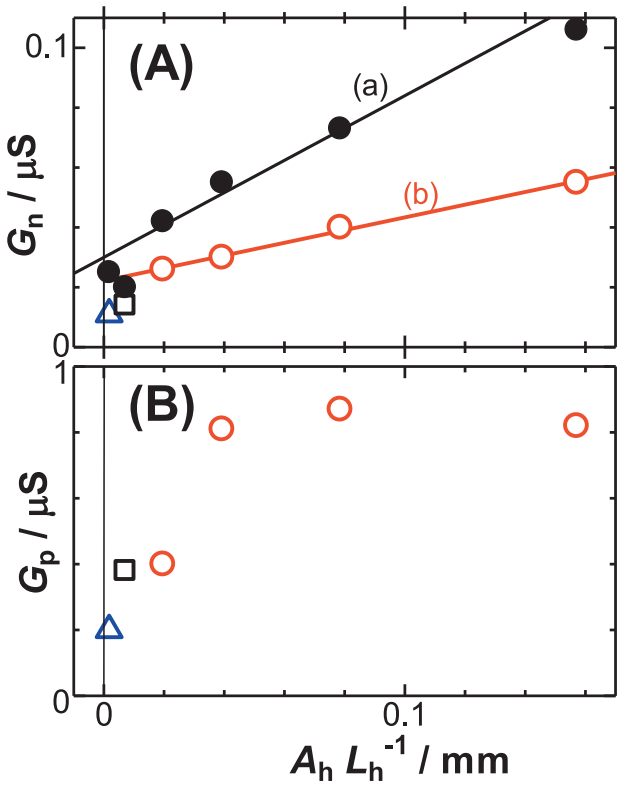

Fig. 3. Variation of the conductance for (A) $V < 0$ and (B) $V > 0$ with the hole dimension, A_h/L_h, in [NaCl] = 0.1 mM, where different marks denote different diameters. Plots (a) and (b) are, respectively, without and with Nafion film.

The second possibility of the electric migration lies in the hole of the PET film. The current density by electric migration of a mono-valent ion with concentration c passing through the pore in length L can be represented by $j = (F^2D/RT)cV_h/L$, where V_h is the voltage applied between inlet and outlet of the hole. The term F^2D/RT is expressed by the molar ionic conductivity, λ, by the Nernst-Einstein equation. When the observed current density is in general assumed to be a sum of the fluxes of the cation and anion, the current through the hole under the charge neutral condition is rewritten as

$$I = A(\lambda_+ + \lambda_-)cV_h/L \quad (1)$$

This equation indicates that the conductance should be proportional to A, $1/L$, and c. Fig. 3(A) shows dependence of conductance, G ($= I/V$), for $V < 0$ on A_h/L_h (b) with and (a) without the Nafion film, where A_h and L_h are the cross section area of the hole and its length. Here G_n is the conductance for $V<0$. Both the plots are approximately linear and converge for small diameters. However, the lines did not pass through the origin, which may indicate leakage currents. We indeed observed 0.01–0.02 μS even for the hole-free PET film. This residual conductance may be caused by leaking current through the edge of the two ground glass flanges. Therefore, this amount of residual conductance was subtracted from the observed conductance for the evaluation of the true conductivity. The slope of plot (a) (without Nafion) was 2.5 times larger than that of plot (b) (with Nafion). The former may be due to transport of both Na^+ and Cl^-, corresponding to $(\lambda_+ + \lambda_-)c$. In contrast, the Nafion film can hinder transport of Cl^-, and hence the conductance is given by λ_+c. The ratio $(\lambda_+ + \lambda_-)/\lambda_+$ calculated for bibliographic values of $\lambda_+ = 5.0 \times 10^{-3}$ S m^2mol^{-1} and $\lambda_- = 7.5 \times 10^{-3}$ S m^2mol^{-1} agrees with the experimental value 2.5. However, the

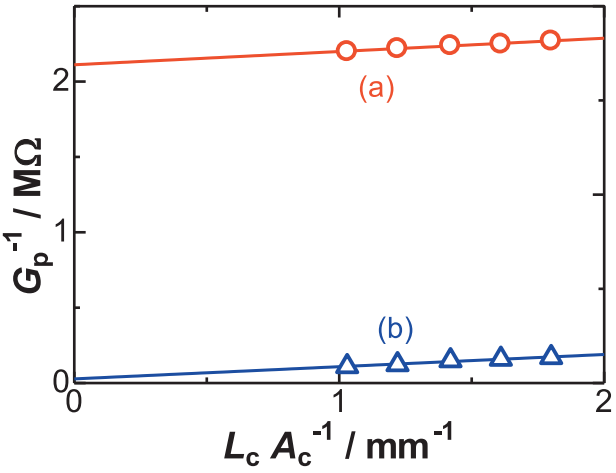

Fig. 4. Variations of $1/G_p$ with L_c/A_c at c_b= 1 mM for (a) without and (b) with the Nafion film for the hole with L_h = 0.05 mm and the diameter 0.05 mm.

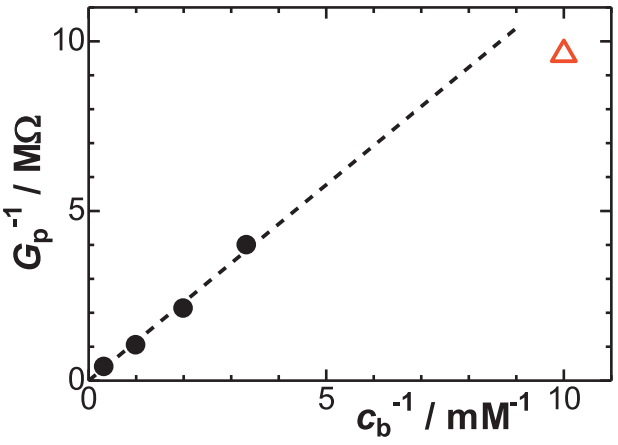

Fig. 5. Dependence of the resistance for $V > 0$ on the inverse of the bulk concentration at the hole 0.05 mm in diameter and 0.1 mm in length.

agreement may be a result of several complications because the dynamic blocking of the Nafion film includes some phenomena other than electrostatic interaction. Fig. 3(B) shows the conductance obtained from the slopes of the voltammograms for $V > 0$, where G_p is the conductance for $V > 0$. The non-linear relation implies invalidity of the electric migration through the hole.

The third possibility of the migration results in ions of bulk solution, which can be measured from voltammograms without the PET or the Nafion film. The voltammograms exhibited behavior consistent with Ohm's law, the slope of which was 0.83 μS for c = 0.1 mM. If A and L in Eq. (1) are replaced by, respectively, the inner area of the glass tube, A_c, and the approximate distance, L_c, between two sensing electrodes (S and R in Fig. 1(A)), the calculated values of $\lambda_+ cLc$ and $(\lambda_+ + \lambda_-)cLc$ are 0.36 μS and 0.89 μS for Lc=72 mm, respectively. The latter is close to the slope (0.83 μS) without the PET or Nafion, indicating that the cell geometry would control G_p. The total resistance between the two electrodes can be regarded as a series combination of the resistance of the hole and that of the cell. The hole resistance with the Nafion is controlled only by the cation because the anion is blocked by the Nafion film, whereas that without the Nafion is both by the cation and the anion. In contrast, the resistance of the cell is determined by the both ions. As a result, we can express the total resistances without and with Nafion as

$$\left(G_p^{-1}\right)_{\text{noNaf}} = (L_h/A_h)/c_b(\lambda_+ + \lambda_-) + (L_c/A_c)/c_b(\lambda_+ + \lambda_-) \quad (2a)$$

$$\left(G_p^{-1}\right)_{\text{Naf}} = (L_h/A_h)/c_+\lambda_+ + (L_c/A_c)/c_b(\lambda_+ + \lambda_-) \quad (2b)$$

where c_b is the concentration of NaCl in the bulk, and c_+ is the concentration of Na^+ at the interface between the Nafion film and the solution in the hole. We measured the *I-V* curves for some values of L_c at a given value of A_c. Fig. 4 shows the variation of obtained G_p^{-1} against L_c/A_c, (a) without and (b) with the Nafion film. The values of the slopes were common (82 Ωm) to (a) and (b), whereas the theoretical value of $1/c_b(\lambda_+ + \lambda_-)$ is 80 Ωm. The evaluation of the common value as well as the agreement with the theoretical value indicates that the carrier of the current should be both ions. The ratio of the intercepts was 77, which may equal $c_+\lambda_+/\{c_b(\lambda_+ + \lambda_-)\}$, according to Eq. (2). Then we have c_+/c_b = 190 or c_+= 0.19 M for c_b = 1 mM of our experimental value. The enhancement of the concentration is caused by the supply of Na^+ from the Nafion film by the cationic flow by the cell-geometric migration.

We plotted $1/G_p$ against $1/c_b$ in Fig. 5. The plot except for the lowest concentration (triangle in Fig. 5) was proportional to $1/c_b$. The proportionality may apparently suggest $(L_h/A_h)/c_+\lambda_+ \approx 0$ from Eq. (2). However, the zero-intercept indicates the proportionality of c_+ to c_b. In other words, the supply of Na^+ from the Nafion film to the hole increases with c_b.

4. Conclusions

The large ($V > 0$, open diode) and the small ($V < 0$, closed diode) conductance of the rectified micro-hole voltammograms are controlled by electric migration effects in both (i) the cell geometry and (ii) the micro-hole geometry, respectively. The open diode current is mostly independent of micro-hole geometry but increases with the ionic concentration in the bulk. The resistance in the micro-hole is not a rate-determining factor because the high conductance is supported by the locally high concentration of Na^+ supplied from the Nafion film (accumulation). A loss of Na^+ in Nafion film can be replenished from the bulk solution in order to maintain electroneutrality. In contrast, the closed diode conductance for $V < 0$ is controlled within the micro-hole geometry and the concentration of the solution bulk, as predicted from the conventional electric migration laws in a cylindrical micro-hole. Therefore, overall the rectification ratio can be enhanced by design of both (i) the cell geometry (area of a cell tube and an electrode distance) and (ii) the micro-hole geometry. These insights will be important for device optimization, especially when designing effective ionic rectifier systems for desalination. Briefly speaking, the rectification effects can be explained in terms of physical variables, i.e. difference in limiting conductances for $V>0$ and $V<0$. Although our elucidation of rectification effects does not include a concept of molecular behavior in the hole, any ionic interaction on molecular scale is not always excluded.

Credit author statement

All authors contributed equally to this manuscript. All authors have read and agreed to the published version of the manuscript.

Supplementary materials

Supplementary material associated with this article can be found, in the online version, at doi:10.1016/j.electacta.2020.136839.

References

[1] H.C. Zhang, Y. Tian, L. Jiang, Fundamental studies and practical applications of bio-inspired smart solid-state nanopores and nanochannels, Nano Today 11 (2016) 61–81.
[2] Z. Slouka, S. Senapati, H.C. Chang, Microfluidic systems with ion-selective membranes, Ann. Rev. Anal. Chem. 7 (2014) 317–335.
[3] B.N. Miles, A.P. Ivanov, K.A. Wilson, F. Dogan, D. Japrung, J.B. Edel, Single molecule sensing with solid-state nanopores: novel materials, methods, and applications, Chem. Soc. Rev. 42 (2013) 15–28.
[4] H.J. Koo, O.D. Velev, Ionic current devices-recent progress in the merging of electronic, microfluidic, and biomimetic structures, Biomicrofluidics 7 (2013) 031501.
[5] D. Wang, G. Wang, Dynamics of ion transport and electric double layer in single conical nanopores, J, Electroanal. Chem. 779 (2016) 39–46.
[6] Y. Rong, Q. Song, K. Mathwig, E. Madrid, F. Marken, pH-induced reversal of ionic diode polarity in 300nm thin membranes based on a polymer of intrinsic microporosity, Electrochem. Commun. 69 (2016) 41–45.
[7] W. Guo, Y. Tian, L. Jiang, Asymmetric ion transport through ion-channel-mimetic solid-state nanopores, Acc. Chem. Res. 46 (2013) 2834–2846.
[8] J.Y. Lin, C.Y. Lin, J.P. Hsu, S. Tseng, Ionic current rectification in a pH-tunable polyelectrolyte brushes functionalized conical nanopore: effect of salt gradient, Anal. Chem. 88 (2016) 1176–1187.
[9] S. Bearden, E. Simpanen, G.G. Zhang, Active current gating in electrically biased conical nanopores, Nanotechnology 26 (2015) 185502.
[10] K. Xiao, G.H. Xie, Z. Zhang, X.Y. Kong, Q. Liu, P. Li, L.P. Wen, L. Jiang, Enhanced stability and controllability of an ionic diode based on funnel-shaped nanochannels with an extended critical region, Adv. Mater. 28 (2016) 3345–3350.
[11] L.L. Wang, H.C. Zhang, Z. Yang, J.J. Zhou, L.P. Wen, L. Li, L. Jiang, Fabrication of hydrogel-coated single conical nanochannel exhibiting controllable ion rectification characteristics, Phys. Chem. Chem. Phys. 17 (2015) 6367–6373.
[12] E. Madrid, P. Cottis, Y.Y. Rong, A.T. Rogers, J.M. Stone, R. Malpass-Evans, M. Carta, N.B. McKeown, F. Marken, Water desalination concept using an ionic rectifier based on a polymer of intrinsic microporosity (PIM), J. Mater. Chem. 3 (2015) 15849–15853.
[13] J. Gao, W. Guo, D. Feng, H. Wang, D. Zhao, L. Jiang, High-performance ionic diode membrane for salinity gradient power generation, J. Am. Chem. Soc. 136 (2014) 12265–12272.
[14] X.Z.J. Hao, B. Bao, Y. Zhou, H. Zhang, J. Pang, Z. Jiang, L. Jiang, Unique ion rectification in hypersaline environment: a high-performance and sustainable power generator system, Sci. Adv. 4 (2018) eaau1665.
[15] J. Han, C. Bae, S. Chae, D. Choi, C. Lee, High-efficiency power generation in hyper-saline environment using conventional nanoporous membrane, Electrochim. Acta 319 (2019) 366–374.
[16] B.R. Putra, E. Madrid, L. Tshwenya, O.A. Arotiba, F. Marken, An AC-driven desalination/salination system based on a Nafion cationic rectifier, Desalination 480 (2020) 114351.
[17] Z.J. Jia, B.G. Wang, S.Q. Song, Y.S. Fan, Blue energy: current technologies for sustainable power generation from water salinity gradient, Renew. Sustain. Energy Rev 31 (2014) 91–100.
[18] Y. Liu, L. Yobas, Cylindrical glass nanocapillaries patterned via coarse lithography (>1μm) for biomicrofluidic applications, Biomicrofluidics 6 (2012) 046502.
[19] L.J. Cheng, L.J. Guo, Nanofluidic diodes, Chem. Soc. Rev. 39 (2010) 923–938.
[20] N.B. McKeown, P.M. Budd, Exploitation of intrinsic microporosity in polymer-based materials, Macromolecules 43 (2010) 5163–5176.
[21] E. Madrid, Y.Y. Rong, M. Carta, N.B. McKeown, R. Malpass-Evans, G.A. Attard, T.J. Clarke, S.H. Taylor, Y.T. Long, F. Marken, Metastable ionic diodes derived from an amine-based polymer of intrinsic microporosity, Angew. Chem. Inter. Ed. 53 (2014) 10751–10754.
[22] E. Madrid, M.A. Buckingham, J.M. Stone, A.T. Rogers, W.J. Gee, A.D. Burrows, P.R. Raithby, V. Celorrio, D.J. Fermin, F. Marken, Ion flow in a zeolitic imidazolate framework results in ionic diode phenomena, Chem. Commun. 52 (2016) 2792–2794.
[23] T. Li, X. He, P. Yu, L. Mao, Nonlinear dependence of the ion current rectification factor on bias voltage in conical nanopipettes, J. Electroanal. Chem. 779 (2016) 106–111.
[24] Y. Wang, Z. Wang, Z. Su, S. Cai, Stretchable and transparent ionic diode and logic gates, Extreme Mechanics Lett 28 (2019) 81–86.
[25] L. Tshwenya, O. Arotiba, B.R. Putra, E. Madrid, K. Mathwig, F. Marken, Cationic diodes by hot-pressing of Fumasep FKS-30 ionomer film onto a microhole in polyethylene terephthalate (PET), J. Electroanal. Chem. 815 (2018) 114–122.
[26] M. Ali, S. Nasir, W. Ensinger, Stereoselective detection of amino acids with protein-modified single asymmetric nanopores, Electrochim. Acta 215 (2016) 231–237.
[27] K. Mathwig, B.D.B. Aaronson, F. Marken, Ionic transport in microhole fluidic diodes based on asymmetric ionomer film deposits, ChemElectroChem 5 (2018) 897–901.
[28] D. He, E. Madrid, B.D.B. Aaronson, L. Fan, J. Doughty, K. Mathwig, A.M. Bond, N.B. McKeown, F. Marken, A cationic diode based on asymmetric Nafion film deposits, ACS Appl. Mater. Interfaces 9 (2017) 11272–11278.
[29] R. Karnik, C. Duan, K. Castelino, H. Daiguji, A. Majumdar, Rectification of ionic current in a nanofluidic diode, Nano Lett. 7 (2007) 547–551.
[30] K. Xiao, L. Chen, Z. Zhang, G. Xie, A tunable ionic diode based on a biomimetic structure-tailorable nanochannel, Angew. Chem. Int. Ed. 129 (2017) 8280–8284.
[31] G.-.C. Liu, M.-.J. Gao, W. Chen, X.-.Y. Hu, Y.-.D. Zhao, pH-modulated ion-current rectification in a cysteine-functionalized glass nanopipette, Electrochem. Commun. 97 (2018) 6–10.
[32] G.-.C. Liu, W. Chen, M.-.J. Gao, L.-.B. Song, Y.-.D. Zhao, Ion-current-rectification-based customizable pH response in glass nanopipettes via silanization, Electrochem. Commun. 93 (2018) 95–99.
[33] W. Khalid, M.A. Abbasi, M. Ali, Z. Ali, W. Ensinger, Zinc ion driven ionic conduction through single asymmetric nanochannels functionalized with nanocomposites, Electrochim. Acta 337 (2020) 135810.
[34] M. Ali, P. Ramirez, S. Nasir, J. Cervera, W. Ensinger, Tetraalkylammonium cations conduction through a single nanofluidic diode: experimental and theoretical studies, Electrochim. Acta 250 (2017) 302–308.
[35] J. Cervera, P. Ramirez, S. Mafe, P. Stroeve, Asymmetric nanopore rectification for ion pumping, electrical power generation, and information processing applications, Electrochim. Acta 56 (2011) 4504–4511.
[36] C. Wei, A.J. Bard, S.W. Feldberg, Current rectification at quartz nanopipet electrodes, Anal. Chem. 69 (1997) 4627–4646.
[37] K. Hu, Y. Wang, H. Cai, M.V. Mirkin, Y. Gao, G. Friedman, Y. Gogotsi, Open carbon nanopipettes as resistive-pulse sensors, rectification sensors, and electrochemical nanoprobes, Anal. Chem. 86 (2014) 8897–8901.
[38] F. Yan, L. Yao, Q. Yang, K. Chen, B. Su, Ionic current rectification by laminated bipolar silica isoporous membrane, Anal. Chem. 91 (2019) 1227–1231.
[39] X. Yin, S. Zhang, Y. Dong, S. Liu, J. Gu, Y. Chen, X. Zhang, X. Zhang, Y. Shao, Ionic current rectification in organic solutions with quartz nanopipettes, Anal. Chem. 87 (2015) 9070–9077.
[40] S. Liu, Y. Dong, W. Zhao, X. Xie, T. Ji, X. Yin, Y. Liu, Z. Liang, D. Momotenko, D. Liang, H.H. Girault, Y. Shao, Studies of ionic current rectification using polyethyleneimines coated glass nanopipettes, Anal. Chem. 84 (2012) 5565–5573.
[41] G. Yossifon, P. Mushenheim, Y.-.C. Chang, H.-.C. Chang, Eliminating the limiting-current phenomenon by geometric field focusing into nanopores and nanoslots, Phys. Rev. Lett. E 81 (2010) 046301, doi:10.1103/PhysRevE.81.046301.
[42] H.-.C. Chang, G. Yossifon, E.A. Demekhin, Nanoscale electrokinetics and microvortices: how microhydrodynamics affects nanofluidic ion flux, Annu. Rev. Fluid Mech. 44 (2012) 401–426, doi:10.1146/annurev-fluid-120710-101046.
[43] G. Yossifon, Y.-.C. Chang, H.-.C. Chang, Rectification, Gating Voltage, and Interchannel Communication of Nanoslot Arrays due to Asymmetric Entrance Space Charge Polarization, Pys. Rev. Lett. 103 (2009) 154502, doi:10.1103/PhysRevLett.103.154502.
[44] R.S. Sorbello, Microscopic driving forces for electromigration, Mater. Res. Soc. Conf. Proc. 427 (1996) 73–81.
[45] B.R. Putra, K.J. Aoki, J. Chen, F. Marken, A cationic rectifier based on a graphene oxide covered microhole: theory and experiment, Langmuir 35 (2019) 2055–2065.